大阪公立大学 Osaka Metropolitan University 学術情報リポジトリ

Amplitude death in delay-coupled oscillators on directed graph

メタデータ	言語: English
	出版者:
	公開日: 2023-03-08
	キーワード (Ja):
	キーワード (En):
	作成者: Sugitani, Yoshiki, Konishi, Keiji
	メールアドレス:
	所属:
URL	http://hdl.handle.net/10466/00017921

Amplitude death in delay-coupled oscillators on directed graphs

Yoshiki Sugitani [1,*] and Keiji Konishi [2]
[1]*Department of Electrical and Electronic Engineering, Ibaraki University 4-12-1 Nakanarusawa, Hitachi, Ibaraki 316-8511, Japan*
[2]*Department of Electrical and Information Systems, Osaka Prefecture University 1-1 Gakuen-cho, Naka-ku, Sakai, Osaka 599-8531, Japan*

(Received 2 February 2022; accepted 6 May 2022; published 3 June 2022)

The present paper investigates amplitude death (AD) in delay-coupled oscillators on directed graphs, in which the connection delays among oscillators are heterogeneous. We reveal that a linear stability analysis of AD can be significantly simplified by focusing on directed cycles in the graph. First, it is proven that the characteristic function of a steady state can be factorized into several functions that can be analyzed independently. Second, we show that the number of connection parameters to be considered for the stability analysis can be reduced, because the stability depends on the sums of connection delays for directed cycles and is independent of the connection delays on edges that do not form directed cycles. The theoretical results are verified through numerical simulations.

DOI: 10.1103/PhysRevE.105.064202

I. INTRODUCTION

Connection delays between oscillators, which are ubiquitous due to the finite velocity of signal propagation [1], can cause various phenomena in coupled oscillators, such as synchronization [2], spatiotemporal patterns [3], oscillation death [4], and clustered chimera states [5]. Amplitude death (AD), which is one such phenomenon, is the stabilization of a homogeneous steady state, i.e., the quenching of oscillations [6–9]. Although this phenomenon can occur without connection delays, it is facilitated by connection delays [10]. From an engineering point of view, AD can be regarded as the suppression of unwanted oscillations. Thus, recently, there have been many studies conducted to apply AD to engineering applications, such as a dc microgrid [11,12], aeroelastic systems [13], and thermoacoustic oscillators [14–18]. On the other hand, from an academic point of view, the influence of various connection delays on AD has received a great deal of attention and has been extensively investigated [7,8,19,20].

Many previous studies on AD in delay-coupled oscillators consider the following two assumptions: (i) all of the connection delays between oscillators are the same (i.e., homogeneous connection delays) and (ii) the network topologies are limited to undirected graphs (i.e., oscillators are coupled bidirectionally). These assumptions can help us to easily analyze the stability of AD theoretically. Specifically, the characteristic function that governs the stability of AD can be factorized into small functions. However, assumptions (i) and (ii) are too idealistic for real engineering systems. Therefore, the manner in which the stability of AD changes when these assumptions are relaxed must be investigated.

There are some studies that consider coupled oscillators without assumption (i), where connection delays between oscillators are not the same. For example, delay-coupled oscillators on a Cartesian product of two subnetworks in which each subnetwork has a different connection delay [21], oscillator networks on a tree graph with asymmetric connection delays [22], and all-to-all oscillators coupled by partial delay connections, in which some oscillators are received as delayed signals from all other oscillators, whereas other oscillators are instantaneously coupled with all other oscillators [23]. These studies [21–23] enable analysis of the stability of AD, even in the absence of assumption (i) using specific network typologies (e.g., Cartesian product, tree graph, or all-to-all). However, the network topologies considered in these previous studies [21–23] are undirected graphs, i.e., assumption (ii) holds. Thus, the network topologies are strongly limited.

A previous study [24] considered delay-coupled oscillators on a one-way ring topology, which do not satisfy assumption (ii), and considered homogeneous connection delays (i.e., assumption (i) is satisfied). In addition, the network topology was restricted to a ring graph. Michiels and Nijmeijer investigated the stability of steady states in delay-coupled oscillators on a general directed graph [25] (i.e., assumption (ii) is not satisfied). However, the connection delays were homogeneous, which means that assumption (i) holds. To our knowledge, there has been no research that deals with AD under the situation in which neither assumption (i) nor assumption (ii) is satisfied.

The present paper investigates AD in delay-coupled oscillators on a general directed graph with heterogeneous connection delays. Neither assumption (i) nor assumption (ii) is satisfied. We reveal that the characteristic function of a steady state can be expressed as the product of several functions by focusing on edges that do not form directed cycles in the directed graph. These functions can be analyzed independently. Furthermore, we show that the stability of AD is independent of connection delays on edges that do not form directed cycles, but is affected by sums of connection delays in directed cycles. These results significantly simplify the

*yoshiki.sugitani.0301@vc.ibaraki.ac.jp

 ©2022 American Physical Society

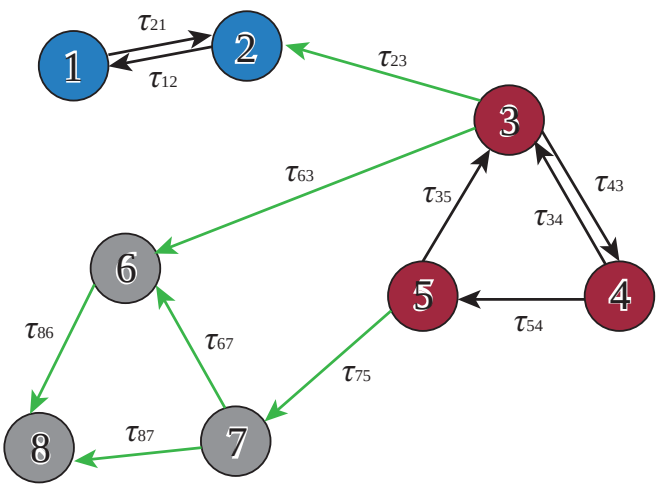

FIG. 1. Delay-coupled oscillators on a directed graph with heterogeneous connection delays ($N = 8$): black edges form directed cycles, and green edges do not form directed cycles.

stability analysis of AD, even under the situation where neither assumption (i) nor assumption (ii) is satisfied.[1] We confirm the theoretical results through numerical simulations.

Throughout the present paper, we use the following notations: $\mathbf{0}_{m,n}$ is the $m \times n$ zero matrix, and $\boldsymbol{I}_m$ is the identity matrix of size m.

II. MATHEMATICAL MODEL

A. Delay-coupled oscillators on a directed graph

We consider N coupled oscillators,

$$\begin{aligned} \dot{\boldsymbol{x}}_i(t) &= \boldsymbol{F}[\boldsymbol{x}_i(t)] + \boldsymbol{b}u_i(t), \\ y_i(t) &= \boldsymbol{c}\boldsymbol{x}_i(t), \end{aligned} \tag{1}$$

where $\boldsymbol{x}_i(t) \in \mathbb{R}^{m\times 1}$ and $y_i(t) \in \mathbb{R}$ $(i \in \{1, \dots, N\})$ are, respectively, the state variable and the output signal of oscillator i. $\boldsymbol{F} : \mathbb{R}^{m\times 1} \to \mathbb{R}^{m\times 1}$ is a nonlinear function that has at least one equilibrium point $\boldsymbol{x}^*$ satisfying $\boldsymbol{F}(\boldsymbol{x}^*) = \mathbf{0}$. Furthermore, $\boldsymbol{b} \in \mathbb{R}^{m\times 1}$ and $\boldsymbol{c} \in \mathbb{R}^{1\times m}$ are the input and output vectors, respectively. Oscillator i receives the input signal,

$$u_i(t) = k\left\{\left[\frac{1}{d_i}\sum_{j=1}^{N} p_{ij}y_j(t-\tau_{ij})\right] - y_i(t)\right\}, \tag{2}$$

where $y_j(t-\tau_{ij})$ is the delayed output signal of oscillator j, τ_{ij} is the connection delay required to propagate the signal from oscillator j to oscillator i (see Fig. 1), and $k \in \mathbb{R}$ is the coupling strength. The adjacency matrix $\{\boldsymbol{P}\}_{ij} := p_{ij} \in \{0, 1\}$ governs the network topology as follows: if there is an edge from oscillator j to oscillator i, $p_{ij} = 1$, otherwise $p_{ij} = 0$. Furthermore, self-feedback is forbidden (i.e., $p_{ii} = 0$). Moreover, $d_i := \sum_{j=1}^{N} p_{ij}$ is the indegree of oscillator i. Assume that each oscillator receives a signal from at least one other oscillator (i.e., $d_i > 0$, $\forall i$).[2] Note that delay-coupled oscillators (1) and (2) can be considered as a generalized model of those considered in a previous study [22], in which oscillators on a undirected tree graph with asymmetric connection delays were investigated.

Coupled oscillators (1) and (2) have the following homogeneous steady state:

$$\left[\boldsymbol{x}_1^T(t)\cdots\boldsymbol{x}_N^T(t)\right]^T = [\boldsymbol{x}^{*T}\cdots\boldsymbol{x}^{*T}]^T. \tag{3}$$

AD can occur when steady state (3) is stable. Linearization of Eqs. (1) and (2) at steady state (3) yields

$$\begin{aligned} \Delta\dot{\boldsymbol{x}}_i(t) &= \boldsymbol{A}\Delta\boldsymbol{x}_i(t) + \boldsymbol{b}\Delta u_i(t), \\ \Delta y_i(t) &= \boldsymbol{c}\Delta\boldsymbol{x}_i(t), \end{aligned} \tag{4}$$

where $\Delta\boldsymbol{x}_i(t) := \boldsymbol{x}_i(t) - \boldsymbol{x}^*$ is a small perturbation, $\boldsymbol{A} := \{d\boldsymbol{F}(\boldsymbol{x})/d\boldsymbol{x}\}_{\boldsymbol{x}=\boldsymbol{x}^*}$ is a Jacobian matrix, and

$$\Delta u_i(t) = k\left[\left(\frac{1}{d_i}\sum_{j=1}^{N} p_{ij}\Delta y_j(t-\tau_{ij})\right) - \Delta y_i(t)\right]. \tag{5}$$

The local stability of steady state (3) is equivalent to the stability of linear system (4) with (5).

B. Frequency domain analysis

The characteristic function of linear system (4) with (5) is given by

$$g(s) = \det[s\boldsymbol{I}_{Nm} - \boldsymbol{I}_N \otimes \bar{\boldsymbol{A}} - k\boldsymbol{E}(s) \otimes \boldsymbol{b}\boldsymbol{c}], \tag{6}$$

where $\bar{\boldsymbol{A}} := \boldsymbol{A} - k\boldsymbol{b}\boldsymbol{c}$, $\boldsymbol{D} := \mathrm{diag}(d_1, \dots, d_N)$, and

$$\boldsymbol{E}(s) := \boldsymbol{D}^{-1}\boldsymbol{T}(s). \tag{7}$$

Here $\{\boldsymbol{T}(s)\}_{ij}$ comprises the connection delay from oscillators j to i as follows: $\{\boldsymbol{T}(s)\}_{ij} = e^{-s\tau_{ij}}$ if $p_{ij} = 1$, otherwise $\{\boldsymbol{T}(s)\}_{ij} = 0$. In other words, $\boldsymbol{T}(s)$ is obtained by replacing the nonzero (i, j) element of $\boldsymbol{P}$ with $e^{-s\tau_{ij}}$, which includes the connection delay τ_{ij} in the edge corresponding to p_{ij}. Thus, matrix $\boldsymbol{T}(s)$ can be considered as the adjacency matrix $\boldsymbol{P}$ with added delay information. Note that $\boldsymbol{E}(s)$ contains information about the network topology and the connection delays. AD can occur [i.e., steady state (3) is locally stable] if and only if all the roots of $g(s) = 0$ have a negative real part. Since the characteristic function (6) can be rewritten as

$$\begin{aligned} g(s) &= \det\begin{bmatrix} s\boldsymbol{I}_{Nm} - \boldsymbol{I}_N \otimes \bar{\boldsymbol{A}} & k\boldsymbol{E}(s) \otimes \boldsymbol{b} \\ \boldsymbol{I}_N \otimes \boldsymbol{c} & \boldsymbol{I}_N \end{bmatrix} \\ &= \det[\boldsymbol{I}_N \otimes (s\boldsymbol{I}_m - \bar{\boldsymbol{A}})] \\ &\quad \times \det\{\boldsymbol{I}_N - k(\boldsymbol{I}_N \otimes \boldsymbol{c})[\boldsymbol{I}_N \otimes (s\boldsymbol{I}_m - \bar{\boldsymbol{A}})]^{-1}(\boldsymbol{E}(s) \otimes \boldsymbol{b})\}, \end{aligned}$$

this function can be simplified as

$$g(s) = [H(s) + kL(s)]^N \hat{g}(s), \tag{8}$$

[1]In Sec. VI we will discuss in detail the differences between our results and those of the componentwise time-shift transformation, which is a useful method for analysis of steady states in delay-coupled oscillators.

[2]The coupling strength k is normalized by d_i in Eq. (2) as in many previous studies on AD [26–28].

where $H(s) := \det[s\boldsymbol{I}_m - \boldsymbol{A}]$, $L(s) := \boldsymbol{c}\,\mathrm{adj}(s\boldsymbol{I}_m - \boldsymbol{A})\boldsymbol{b}$,

$$\hat{g}(s) := \det[\boldsymbol{I}_N - kG(s)\boldsymbol{E}(s)], \tag{9}$$

$$G(s) := \frac{L(s)}{H(s) + kL(s)}. \tag{10}$$

Note that $L(s)/H(s)$ denotes the transfer function for linear system (4) from $\Delta u_i(t)$ to $\Delta y_i(t)$, and $G(s)$ is the transfer function for linear system (4) with a nondelayed self-feedback $\Delta u_i(t) = k\Delta y_i(t)$.

The first factor on the right-hand side in Eq. (8), $\{H(s) + kL(s)\}^N$, denotes the characteristic function for linear system (4) with nondelayed self-feedback [see the denominator of $G(s)$ in Eq. (10)]. The second factor in Eq. (8), $\hat{g}(s)$, contains information about the network topology and connection delays, $\boldsymbol{E}(s)$. For steady state (3) to be stable, both factors must be stable [i.e., all the roots of $H(s) + kL(s) = 0$ and $\hat{g}(s) = 0$ must have a negative real part]. The stability analysis of $\hat{g}(s)$ is more difficult, because $\hat{g}(s)$ is a transcendental function due to the connection delays.

Before analyzing $\hat{g}(s)$ with a general directed graph, we present a specific example of $\hat{g}(s)$ with the simple network shown in Fig. 1. This network has eight oscillators and 12 different connection delays. The characteristic function $\hat{g}(s)$ for this network is simply given by

$$\hat{g}(s) = \left[1 - \frac{k^2}{2}G(s)^2 e^{-s(\tau_{12}+\tau_{21})}\right] \times \left[1 - \frac{k^3}{2}G(s)^3 e^{-s(\tau_{54}+\tau_{43}+\tau_{35})} - \frac{k^2}{2}G(s)^2 e^{-s(\tau_{34}+\tau_{43})}\right]. \tag{11}$$

Equation (11) has the following features: (I) the equation is factorized into two simple functions; (II) the sums of the connection delays for all directed cycles (i.e., delays on black edges in Fig. 1) are included, i.e., the cycle $\{2, 1, 2\}$ (i.e., $\tau_{12} + \tau_{21}$), the cycle $\{4, 5, 3, 4\}$ (i.e., $\tau_{54} + \tau_{43} + \tau_{35}$), and the cycle $\{4, 3, 4\}$ (i.e., $\tau_{34} + \tau_{43}$); and (III) connection delays on edges that do not form directed cycles (i.e., delays on green edges in Fig. 1) are not included. As a result, for the network topology shown in Fig. 1, $\hat{g}(s)$ is given by the product of the simple functions, and its stability depends only on the sums of connection delays in certain edges. In other words, the above features indicate that the stability analysis of $\hat{g}(s)$ can be simplified for the following reasons: the factorized functions (i.e., the first and second factors in Eq. (11)) can be analyzed independently; and the number of connection parameters to be analyzed is significantly reduced, i.e., only four in Eq. (11) (i.e., k, $\tau_{12} + \tau_{21}$, $\tau_{54} + \tau_{43} + \tau_{35}$, and $\tau_{34} + \tau_{43}$), even though the network in Fig. 1 has 12 different connection delays.

In Secs. III and IV, we show that features (I), (II), and (III) above can be confirmed, even for a general directed graph.

III. FACTORIZATION OF CHARACTERISTIC FUNCTION

This section considers feature (I) on a general directed graph. First, in Sec. III A we show that the characteristic function $\hat{g}(s)$ on a directed graph can be factorized into two characteristic functions corresponding to two subgraphs in the directed graph. It is shown that these factorized functions can be further factorized by similar operations. Second, Sec. III B focuses on the factorized functions that correspond to acyclic graphs. Finally, the above results are summarized as a main theorem in Sec. III C.

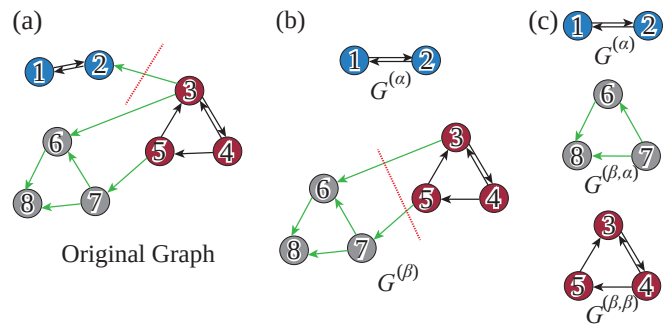

FIG. 2. Separation of the graph shown in Fig. 1 based on Lemma 1. The red dashed lines denote the edges that separate one graph into two subgraphs. (a) Original graph; (b) original graph separated into $G^{(\alpha)}$ and $G^{(\beta)}$; and (c) $G^{(\beta)}$ separated into $G^{(\beta,\alpha)}$ and $G^{(\beta,\beta)}$.

A. Partitioning graph

The function $\hat{g}(s)$ for a general directed graph can be factorized into two functions as follows.

Lemma 1. Consider delay-coupled oscillators (1) and (2) on a directed graph. Assume that the directed graph can be partitioned into two subgraphs $G^{(\alpha)}$ with $N^{(\alpha)}$ nodes and $G^{(\beta)}$ with $N^{(\beta)}$ nodes, in which there exist at least an edge from $G^{(\beta)}$ to $G^{(\alpha)}$ and no edges from $G^{(\alpha)}$ to $G^{(\beta)}$. The characteristic function $\hat{g}(s)$ can be factorized as

$$\hat{g}(s) = g^{(\alpha)}(s)g^{(\beta)}(s), \tag{12}$$

where

$$g^{(\alpha)}(s) := \det\left[\boldsymbol{I}_{N^{(\alpha)}} - kG(s)\boldsymbol{E}^{(\alpha)}(s)\right], \tag{13}$$

$$g^{(\beta)}(s) := \det\left[\boldsymbol{I}_{N^{(\beta)}} - kG(s)\boldsymbol{E}^{(\beta)}(s)\right]. \tag{14}$$

Matrix $\boldsymbol{E}^{(\alpha)}(s) \in \mathbb{C}^{N^{(\alpha)}\times N^{(\alpha)}}$ [$\boldsymbol{E}^{(\beta)}(s) \in \mathbb{C}^{N^{(\beta)}\times N^{(\beta)}}$] is obtained by removing rows and columns corresponding to the edges to and from nodes in $G^{(\beta)}$ ($G^{(\alpha)}$) from $\boldsymbol{E}(s)$.

Proof. See Appendix A. ■

For instance, the graph shown in Fig. 1 can be partitioned into a subgraph $G^{(\alpha)}$ with two nodes and another subgraph $G^{(\beta)}$ with six nodes, as shown in Figs. 2(a) and 2(b), and there exists only one edge from $G^{(\beta)}$ to $G^{(\alpha)}$. Furthermore, $\boldsymbol{E}(s)$ for

the graph in Fig. 1 is given by

$$\boldsymbol{E}(s)=\left(\begin{array}{cc|cccccc} 0 & e^{-s\tau_{12}} & 0 & 0 & 0 & 0 & 0 & 0 \\ \frac{e^{-s\tau_{21}}}{2} & 0 & \frac{e^{-s\tau_{23}}}{2} & 0 & 0 & 0 & 0 & 0 \\ \hline 0 & 0 & 0 & \frac{e^{-s\tau_{34}}}{2} & \frac{e^{-s\tau_{35}}}{2} & 0 & 0 & 0 \\ 0 & 0 & e^{-s\tau_{43}} & 0 & 0 & 0 & 0 & 0 \\ 0 & 0 & 0 & e^{-s\tau_{54}} & 0 & 0 & 0 & 0 \\ 0 & 0 & \frac{e^{-s\tau_{63}}}{2} & 0 & 0 & 0 & \frac{e^{-s\tau_{67}}}{2} & 0 \\ 0 & 0 & 0 & 0 & e^{-s\tau_{75}} & 0 & 0 & 0 \\ 0 & 0 & 0 & 0 & 0 & \frac{e^{-s\tau_{86}}}{2} & \frac{e^{-s\tau_{87}}}{2} & 0 \end{array}\right). \tag{15}$$

The $i \in \{1,\ldots,8\}$th row (column) of $\boldsymbol{E}(s)$ corresponds to edges to (from) node i. We see that the first and second (third to eighth) rows and columns correspond to edges to and from nodes in $G^{(\alpha)}$ ($G^{(\beta)}$). For example, the (1,2) element of matrix (15) corresponds to the edge from node 2 to node 1 in $G^{(\alpha)}$. Therefore, Eq. (9) with Eq. (15) can be factorized into Eqs. (13) and (14) with

$$\boldsymbol{E}^{(\alpha)}(s)=\begin{pmatrix} 0 & e^{-s\tau_{12}} \\ e^{-s\tau_{21}}/2 & 0 \end{pmatrix}, \tag{16}$$

$$\boldsymbol{E}^{(\beta)}(s)=\left(\begin{array}{ccc|ccc} 0 & e^{-s\tau_{34}}/2 & e^{-s\tau_{35}}/2 & 0 & 0 & 0 \\ e^{-s\tau_{43}} & 0 & 0 & 0 & 0 & 0 \\ 0 & e^{-s\tau_{54}} & 0 & 0 & 0 & 0 \\ \hline e^{-s\tau_{63}}/2 & 0 & 0 & 0 & e^{-s\tau_{67}}/2 & 0 \\ 0 & 0 & e^{-s\tau_{75}} & 0 & 0 & 0 \\ 0 & 0 & 0 & e^{-s\tau_{86}}/2 & e^{-s\tau_{87}}/2 & 0 \end{array}\right), \tag{17}$$

where $\boldsymbol{E}^{(\alpha)}(s)$ in Eq. (16) ($\boldsymbol{E}^{(\beta)}(s)$ in Eq. (17)) is obtained by removing the third to eighth (first and second) rows and columns corresponding to edges to and from nodes in $G^{(\beta)}$ ($G^{(\alpha)}$) from matrix (15). We can confirm that Eq. (13) with Eq. (16) is the first factor on the right-hand side of Eq. (11).

Let us focus on $\boldsymbol{E}^{(\alpha)}(s)$ in Eq. (16). Since $\boldsymbol{E}^{(\alpha)}(s)$ is obtained by removing rows and columns from $\boldsymbol{E}(s)$ in Eq. (15) [the general form of which is given by Eq. (7)], $\boldsymbol{E}^{(\alpha)}(s)$ can be written as

$$\boldsymbol{E}^{(\alpha)}(s)=\begin{pmatrix} 1 & 0 \\ 0 & 2 \end{pmatrix}^{-1}\begin{pmatrix} 0 & e^{-s\tau_{12}} \\ e^{-s\tau_{21}} & 0 \end{pmatrix}, \tag{18}$$

where the first factor is the inverse matrix of the degree matrix of nodes belonging to $G^{(\alpha)}$ in the original graph [see nodes 1 and 2 in Figs. 2(a) and 2(b)], and the second factor is obtained by replacing the nonzero elements of the adjacency matrix $\left(\begin{smallmatrix} 1 & 0 \\ 0 & 1 \end{smallmatrix}\right)$ of $G^{(\alpha)}$ with the connection delays.

For a general network topology, let $V^{(\alpha)}=\{v_1^{(\alpha)},\ldots,v_{N^{(\alpha)}}^{(\alpha)}\}$ be the set of nodes in $G^{(\alpha)}$, where $v_j^{(\alpha)}\in\{1,\ldots,N\}$ with $j=1,\ldots,N^{(\alpha)}$ is the jth node in $G^{(\alpha)}$. Then $\boldsymbol{E}^{(\alpha)}(s)$ in Eq. (13) can be described as

$$\boldsymbol{E}^{(\alpha)}(s):=\boldsymbol{D}^{(\alpha)^{-1}}\boldsymbol{T}^{(\alpha)}(s), \tag{19}$$

where $\boldsymbol{D}^{(\alpha)}:=\mathrm{diag}\big(d_{v_1^{(\alpha)}},\ldots,d_{v_{N^{(\alpha)}}^{(\alpha)}}\big)$ is the degree matrix of nodes in $V^{(\alpha)}$ of the original graph, and $\boldsymbol{T}^{(\alpha)}(s)\in\mathbb{C}^{N^{(\alpha)}\times N^{(\alpha)}}$ comprises the adjacency matrix $\boldsymbol{P}^{(\alpha)}\in\mathbb{R}^{N^{(\alpha)}\times N^{(\alpha)}}$ of $G^{(\alpha)}$ and the connection delays in $G^{(\alpha)}$, in which $\{\boldsymbol{P}^{(\alpha)}\}_{ij}=1$ if there is an edge from node $v_j^{(\alpha)}$ to node $v_i^{(\alpha)}$, and otherwise $\{\boldsymbol{P}^{(\alpha)}\}_{ij}=0$. Specifically, $\{\boldsymbol{T}^{(\alpha)}(s)\}_{ij}$ contains the connection delay from node $v_j^{(\alpha)}$ to node $v_i^{(\alpha)}$ as follows: $\{\boldsymbol{T}^{(\alpha)}(s)\}_{ij}=e^{-s\tau_{v_i^{(\alpha)}v_j^{(\alpha)}}}$ if $\{\boldsymbol{P}^{(\alpha)}\}_{ij}=1$, otherwise $\{\boldsymbol{T}^{(\alpha)}(s)\}_{ij}=0$. Hence, matrix $\boldsymbol{T}^{(\alpha)}(s)$ can be considered as the adjacency matrix $\boldsymbol{P}^{(\alpha)}$ with added delay information. The same applies to $\boldsymbol{E}^{(\beta)}(s)$ in Eq. (14). Thus, $\boldsymbol{E}^{(\alpha)}(s)$ and $\boldsymbol{E}^{(\beta)}(s)$ in Eqs. (13) and (14) corresponding to subgraphs $G^{(\alpha)}$ and $G^{(\beta)}$ have a similar form to $\boldsymbol{E}(s)$ of Eq. (7) in Eq. (9) corresponding to the original graph. Therefore, if graph $G^{(\alpha)}$ ($G^{(\beta)}$) can be further partitioned into two subgraphs $G^{(\alpha,\alpha)}$ and $G^{(\alpha,\beta)}$ ($G^{(\beta,\alpha)}$ and $G^{(\beta,\beta)}$), and there exist edges only from $G^{(\alpha,\beta)}$ to $G^{(\alpha,\alpha)}$ ($G^{(\beta,\beta)}$ to $G^{(\beta,\alpha)}$), then we can factorize $g^{(\alpha)}(s)$ ($g^{(\beta)}(s)$) by Lemma 1.

For example, subgraph $G^{(\beta)}$ in Fig. 2(b) can be partitioned into two subgraphs: Subgraph $G^{(\beta,\alpha)}$ with nodes 6, 7, 8 and subgraph $G^{(\beta,\beta)}$ with nodes 3, 4, 5, as shown in Fig. 2(c). Furthermore, we can confirm that there exist edges only from $G^{(\beta,\beta)}$ to $G^{(\beta,\alpha)}$ in $G^{(\beta)}$. Thus, based on Lemma 1, $g^{(\beta)}(s)$ with Eq. (17) can be factorized as

$$\begin{aligned} g^{(\beta)}(s) &= g^{(\beta,\alpha)}(s)g^{(\beta,\beta)}(s) \\ &= \det\big[\boldsymbol{I}_3-kG(s)\boldsymbol{E}^{(\beta,\alpha)}(s)\big]\det\big[\boldsymbol{I}_3-kG(s)\boldsymbol{E}^{(\beta,\beta)}(s)\big], \end{aligned} \tag{20}$$

where

$$\boldsymbol{E}^{(\beta,\alpha)}(s):=\begin{pmatrix} 0 & e^{-s\tau_{67}}/2 & 0 \\ 0 & 0 & 0 \\ e^{-s\tau_{86}}/2 & e^{-s\tau_{87}}/2 & 0 \end{pmatrix}, \tag{21}$$

$$\boldsymbol{E}^{(\beta,\beta)}(s):=\begin{pmatrix} 0 & e^{-s\tau_{34}}/2 & e^{-s\tau_{35}}/2 \\ e^{-s\tau_{43}} & 0 & 0 \\ 0 & e^{-s\tau_{54}} & 0 \end{pmatrix}. \tag{22}$$

Matrix (21) [matrix (22)] is obtained by removing rows and columns corresponding to edges of nodes 3, 4, 5 (6, 7, 8) from $\boldsymbol{E}^{(\beta)}(s)$ in Eq. (17), i.e., by removing the first, second, and third (fourth, fifth, and sixth) rows and columns from matrix (17).

We can confirm that if there are edges only from one subgraph to another subgraph, these edges do not form directed cycles (see green edges in Fig. 1). Thus, based on Lemma 1, we can continue to factorize the characteristic functions by a similar operation, as long as their corresponding subgraphs have edges that do not form directed cycles (i.e., green edges). Section III B considers the specific factorized functions.

B. Characteristic function for an acyclic graph

Here we consider the case in which the factorized function $g^{(\alpha)}(s)$ in Eq. (13) has $\boldsymbol{E}^{(\alpha)}(s)$, which corresponds to acyclic graph $G^{(\alpha)}$. Then $g^{(\alpha)}(s)$ can be calculated as follows.

Lemma 2. If matrix $\boldsymbol{E}^{(\alpha)}(s)$ in Eq. (19) corresponds to an acyclic graph, then Eq. (13) is reduced to $g^{(\alpha)}(s) = 1$.

Proof. See Appendix B. ■

Note that Lemma 2 can also be applied to Eq. (14), if $\boldsymbol{E}^{(\beta)}(s)$ is the adjacency matrix corresponding to an acyclic graph. For instance, in Fig. 2(c), graph $G^{(\beta,\alpha)}$ is an acyclic graph. Thus, we can obtain $g^{(\beta,\alpha)}(s) = 1$ in Eq. (20) according to Lemma 2, which leads to

$$g^{(\beta)}(s) = g^{(\beta,\beta)}(s). \tag{23}$$

Equation (23) is equivalent to the second factor of the right-hand side in Eq. (11).

Consequently, $\hat{g}(s)$ for the graph shown in Fig. 1 can be described as the product of two characteristic functions corresponding to subgraphs $G^{(\alpha)}$ and $G^{(\beta,\beta)}$, as shown in Eq. (11). Lemmas 1 and 2 show that characteristic function $\hat{g}(s)$ can be factorized by focusing on edges that do not form directed cycles.

C. Factorization of characteristic functions

In order to summarize the results in the preceding subsections, assume that a directed graph is divided into M subgraphs after repeated partitioning by focusing on edges that do not form directed cycles. In other words, assume that M subgraphs are obtained by removing all edges that do not form directed cycles from the original graph (e.g., $M = 2$ for the graph shown in Fig. 1). Let $V_q := \{v_{q,1}, \ldots, v_{q,N_q}\}$ be the set of nodes in qth subgraph with N_q nodes, where $v_{q,i} \in \{1, \ldots, N\}$ $(i = 1, \ldots, N_q)$ is the ith node in qth subgraph. From Lemmas 1 and 2, $\hat{g}(s)$ can be described by $\hat{g}(s) = \prod_{q=1}^{M} g_q(s)$ with

$$g_q(s) := \det\left[\boldsymbol{I}_{N_q} - kG(s)\boldsymbol{D}_q^{-1}\boldsymbol{T}_q(s)\right], \tag{24}$$

where $\boldsymbol{D}_q := \mathrm{diag}\left(d_{v_{q,1}}, \ldots, d_{v_{q,N_q}}\right)$ is the degree matrix of nodes in V_q of the original directed graph. Here $\boldsymbol{T}_q(s) \in \mathbb{C}^{N_q \times N_q}$ composes the adjacency matrix $\boldsymbol{P}_q \in \mathbb{R}^{N_q \times N_q}$ of the qth subgraph and the connection delays in qth subgraph, in which $\{\boldsymbol{P}_q\}_{ij} = 1$ if there is an edge from node $v_{q,j}$ to node $v_{q,i}$, otherwise $\{\boldsymbol{P}_q\}_{ij} = 0$. Specifically, $\{\boldsymbol{T}_q(s)\}_{ij}$ contains the connection delay from node $v_{q,j}$ to node $v_{q,i}$: $\{\boldsymbol{T}_q(s)\}_{ij} = e^{-s\tau_{v_{q,i}v_{q,j}}}$ if $\{\boldsymbol{P}_q\}_{ij} = 1$, otherwise $\{\boldsymbol{T}_q(s)\}_{ij} = 0$. In other words, $\boldsymbol{T}_q(s)$ is obtained by replacing the nonzero (i, j) element of $\boldsymbol{P}_q$ by $e^{-s\tau_{v_{q,i}v_{q,j}}}$. We see that the characteristic function $g_q(s)$ corresponds to qth subgraph. Then we summarize the results as follows.

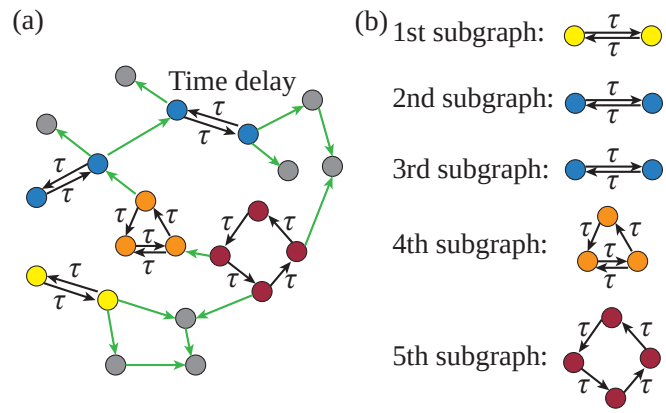

FIG. 3. Delay-coupled oscillators: (a) $N = 21$ oscillators, where all edges that form directed cycles (black edges) have a connection delay τ; (b) $M = 5$ subgraphs obtained by removing all green edges in (a).

Theorem 1. Consider delay-coupled oscillators (1) and (2) on a directed graph. The local stability of steady state (3) is governed by the characteristic function,

$$g(s) = \{H(s) + kL(s)\}^N \prod_{q=1}^{M} g_q(s), \tag{25}$$

where $g_q(s)$ is defined by Eq. (24).

Proof. The proof is obvious from Lemmas 1 and 2 and the above discussion. The proof is therefore omitted. ■

From Theorem 1, the stability of $g(s)$ can be reduced to that of each element $g_q(s)$ that can be analyzed independently. For example, let us consider the graph with $N = 21$ oscillators shown in Fig. 3(a). Edges that form (do not form) directed cycles are indicated in black (green). For simplicity, assume that all connection delays in the edges that form directed cycles are fixed at τ [see black edges in Fig. 3(a)]. The other edges, the green edges in Fig. 3(a), are assumed to have arbitrary connection delays. We can obtain $M = 5$ subgraphs by removing all edges that do not form directed cycles (i.e., green edges), as shown in Fig. 3(b). Thus, according to Theorem 1, the characteristic function for the graph in Fig. 3(a) is given by

$$g(s) = [H(s) + kL(s)]^{21} g_1(s)g_2(s)g_3(s)g_4(s)g_5(s), \tag{26}$$

where $g_q(s)$ $(q = 1, \ldots, 5)$ corresponds to the characteristic function for the qth subgraph shown in Fig. 3(b) and is given by Eq. (24) with $\boldsymbol{D}_1 = \mathrm{diag}(1, 1)$, $\boldsymbol{D}_{2,3} = \mathrm{diag}(2, 1)$ $\boldsymbol{D}_4 = \mathrm{diag}(1, 2, 2)$, $\boldsymbol{D}_5 = \mathrm{diag}(1, 1, 1, 1)$,

$$\boldsymbol{T}_1(s) = \boldsymbol{T}_{2,3}(s) = e^{-s\tau}\begin{pmatrix} 0 & 1 \\ 1 & 0 \end{pmatrix},$$

$$\boldsymbol{T}_4(s) = e^{-s\tau}\begin{pmatrix} 0 & 0 & 1 \\ 1 & 0 & 1 \\ 0 & 1 & 0 \end{pmatrix},$$

$$\boldsymbol{T}_5(s) = e^{-s\tau}\begin{pmatrix} 0 & 0 & 0 & 1 \\ 1 & 0 & 0 & 0 \\ 0 & 1 & 0 & 0 \\ 0 & 0 & 1 & 0 \end{pmatrix}.$$

Note that the first [yellow in Fig. 3(b)], second, and third subgraphs [blue in Fig. 3(b)] are recognized as different subgraphs. This is because one of the nodes in the second and third subgraphs has indegree two in the original graph [blue in Fig. 3(a)], but all nodes in the first subgraph have indegree one in the original graph. Therefore, the first diagonal element of $\boldsymbol{D}_{2,3}$ is two, whereas that of $\boldsymbol{D}_1$ is one.

IV. REDUCTION OF THE NUMBER OF CONNECTION PARAMETERS

This section focuses on features (II) and (III), which indicate that the number of connection parameters to be analyzed for AD can be reduced. Calculating the determinant of Eq. (9) yields the following result.

Corollary 1. Consider delay-coupled oscillators (1) and (2) on a directed graph. The local stability of steady state (3) depends not on each connection delay, but rather on the sums of the connection delays in directed cycles, which are subgraphs of the directed graph.

Proof. See Appendix C. ■

For example, for the network in Fig. 1, the characteristic function (11) is dependent on the sums of the connection delays in the three closed cycles. Corollary 1 can be regarded as the extended version of Lemma 1 in our previous study [22] that considers only undirected tree graphs.

Furthermore, from Corollary 1, we can straightforwardly obtain the following result.

Corollary 2. The connection delays on edges that do not form directed cycles are independent of the stability of steady state (3).

Proof. The proof is omitted, since it is obvious from Corollary 1. ■

For instance, both characteristic functions in Eqs. (11) and (26) do not include the connection delays for green edges in Figs. 1 and 3(a).

Corollaries 1 and 2 show that the stability of $\hat{g}(s)$ depends on the sums of the connection delays in directed cycles. The stability is independent of the connection delays on edges that do not form directed cycles. As a result, the number of connection parameters to be considered can be reduced significantly. Corollary 2 indicates that, in order to induce AD, we can freely set the connection delays on edges that do not form a directed cycle. This result may be useful for engineering applications in which the connection delays are limited due to physical constraints.

In Secs. III and IV we showed the following results. The characteristic function can be factorized by focusing on edges that do not form directed cycles (i.e., Theorem 1). The stability of steady state (3) is affected by the sums of connection delays on edges of the directed cycles (i.e., Corollary 1) and is not affected by connection delays on edges that do not form directed cycles (i.e., Corollary 2). These results simplify the stability analysis of AD, even with directed graphs and heterogeneous connection delays.

V. NUMERICAL EXAMPLES

This section numerically confirms the analytical results provided in the previous sections. We consider Rössler oscillators [29] described by Eq. (1) with

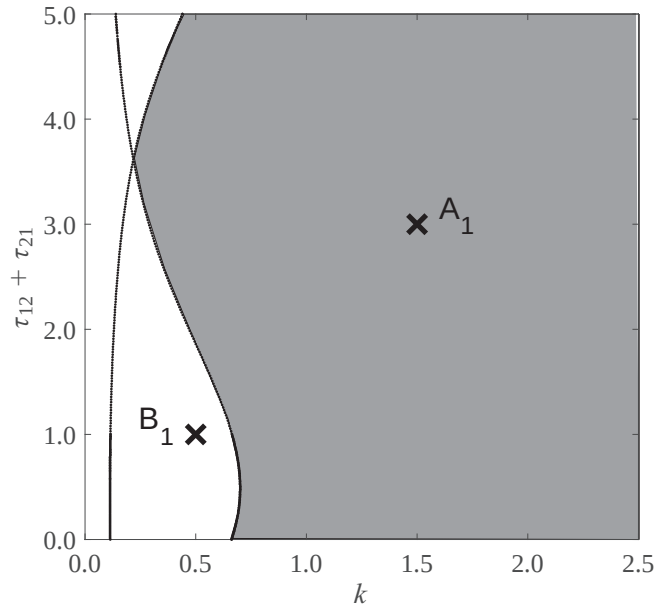

FIG. 4. Marginal stability curves (black lines) and stability region (gray area) for $g_1(s)$, the first factor on the right-hand side in Eq. (11), on $(k, \tau_{12}+\tau_{21})$ space.

$$\boldsymbol{F}(\boldsymbol{x}) = \begin{bmatrix} -x^{(2)} - x^{(3)} \\ x^{(1)} + ax^{(2)} \\ b + x^{(3)}(x^{(1)} - c) \end{bmatrix}, \quad \boldsymbol{b} = \begin{bmatrix} 1 \\ 0 \\ 0 \end{bmatrix}, \quad \boldsymbol{c} = \begin{bmatrix} 1 \\ 0 \\ 0 \end{bmatrix}^T, \tag{27}$$

where $a = 0.2$, $b = 0.2$, and $c = 5.7$ [29]. There exist two equilibrium points satisfying $\boldsymbol{F}(\boldsymbol{x}^*_\pm) = \boldsymbol{0}$,

$$\boldsymbol{x}^*_\pm := [aX_\pm,\ -X_\pm,\ X_\pm]^T, \tag{28}$$

where $X_\pm := (c \pm \sqrt{c^2 - 4ab})/(2a)$. We focus only on the stability of $\boldsymbol{x}^*_-$, because $\boldsymbol{x}^*_+$ satisfies the odd number property, under which AD never occurs for undirected graphs [30]. The network topology shown in Fig. 1 is considered throughout this section.

From Theorem 1, the characteristic function $g(s)$ is factorized into three factors,

$$g(s) = [H(s) + kL(s)]^8 g_1(s) g_2(s), \tag{29}$$

where $g_1(s)$ and $g_2(s)$ are equivalent to the first and second factors on the right-hand side in Eq. (11), respectively. In other words, $g_1(s)$ and $g_2(s)$ are the characteristic functions corresponding to graphs $G^{(\alpha)}$ and $G^{(\beta,\beta)}$ in Fig. 2(c). Note that the number of connection parameters to be considered in Eq. (29) is only four (i.e., k, $\tau_{12}+\tau_{21}$, $\tau_{34}+\tau_{43}$, and $\tau_{54}+\tau_{43}+\tau_{35}$), although the network in Fig. 1 has 12 different connection delays.

Let us consider the three factors in Eq. (29), $H(s) + kL(s)$, $g_1(s)$, and $g_2(s)$, separately. The Routh-Hurwitz stability criterion indicates that the first factor $H(s) + kL(s)$ is stable for $0.2 < k < 5.0$. Figure 4 shows the stability region (i.e., gray area) for the second factor $g_1(s)$ in Eq. (29) on $(k, \tau_{12}+\tau_{21})$ parameter space. The black lines denote the marginal stability curves on which a root for $g_1(s) = 0$ is on the imaginary axis

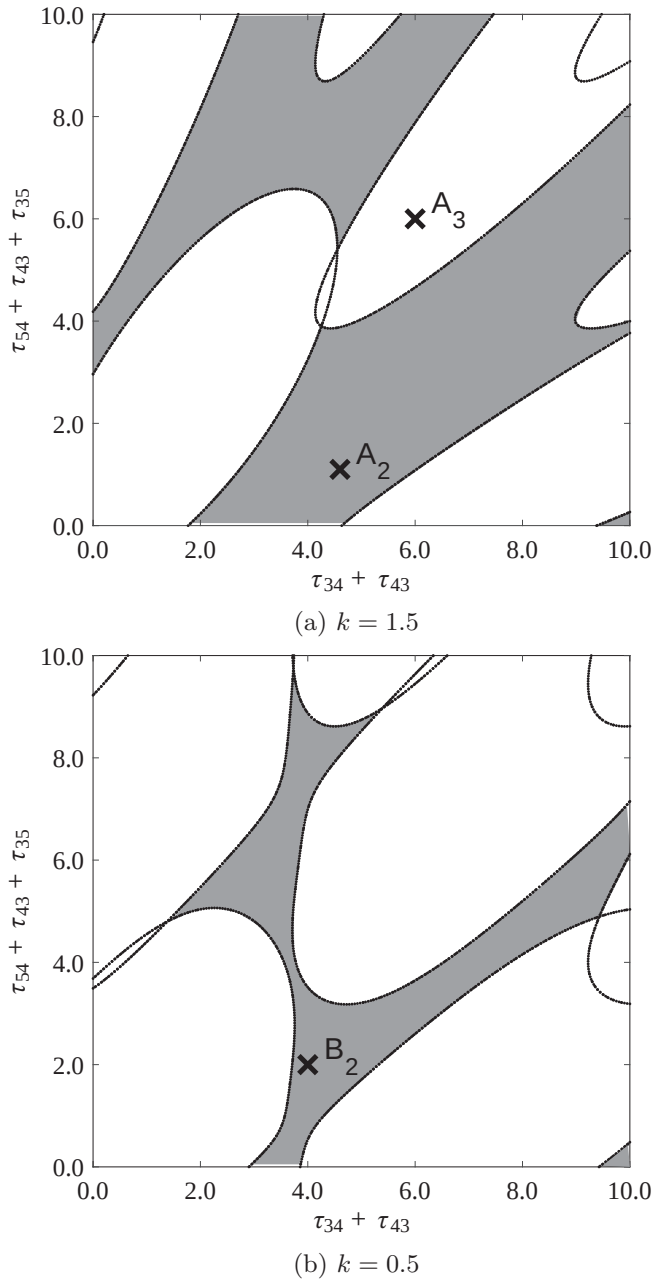

FIG. 5. Marginal stability curves (black lines) and stability region (gray area) for $g_2(s)$, the second factor on the right-hand side in Eq. (11), on $(\tau_{34}+\tau_{43}, \tau_{54}+\tau_{43}+\tau_{35})$ space: (a) $k = 1.5$, (b) $k = 0.5$.

[8]. In the stability region, the real part of the dominant root for $g_1(s) = 0$ is negative. Note that the vertical axis is the sum of the delays $\tau_{12}+\tau_{21}$, but not each delay. The third factor $g_2(s)$ in Eq. (29) has three connection parameters k, $\tau_{34}+\tau_{43}$, and $\tau_{54}+\tau_{43}+\tau_{35}$. We fix k and numerically calculate the stability of $g_2(s)$ on $(\tau_{34}+\tau_{43},\ \tau_{54}+\tau_{43}+\tau_{35})$ parameter space. Figures 5(a) and 5(b) show the stability regions for $k = 1.5$ and 0.5, respectively.

In order to perform numerical simulations, we set the coupling strength to $k = 1.5$ and the connection

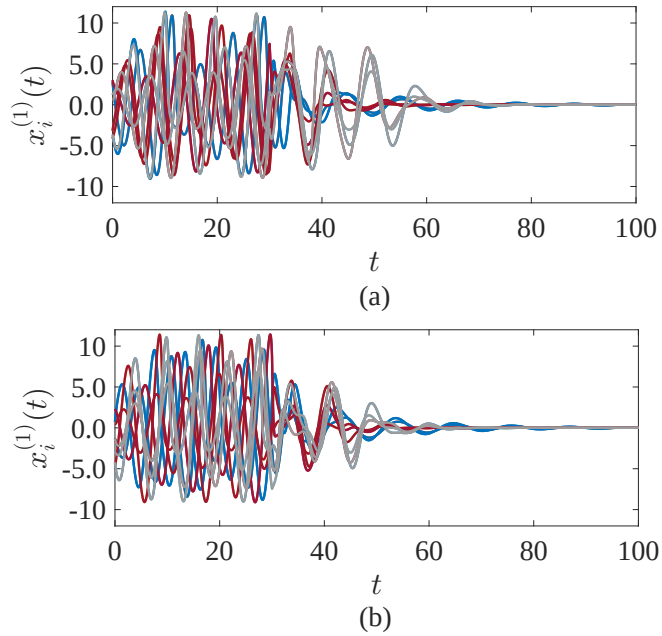

FIG. 6. Time series data for Rössler oscillators with the network topology shown in Fig. 1. The coupling parameters correspond to point A1 in Fig. 4 and point A2 in Fig. 5(a): (a) connection delays (31), (b) connection delays (32).

delays to

$$\tau_{12}+\tau_{21} = 3.0,\ \ \tau_{34}+\tau_{43} = 4.6,\ \ \tau_{54}+\tau_{43}+\tau_{35} = 1.1, \tag{30}$$

which correspond to the connection parameters at point A1 in Fig. 4 and point A2 in Fig. 5(a). Then all three factors $H(s)+kL(s)$, $g_1(s)$, and $g_2(s)$ in Eq. (29) are stable, i.e., $g(s)$ is stable. Figure 6(a) shows the time series data for $x^{(1)}(t)$ for all oscillators, oscillators i ($i = 1, \ldots, 8$), with these connection parameters. Connection delays used in Fig. 6(a) are set to

$$\begin{aligned}&\tau_{12} = 1.3,\ \ \tau_{21} = 1.7,\ \ \tau_{34} = 3.8,\ \ \tau_{43} = 0.8,\ \ \tau_{54} = 0.2,\\ &\tau_{35} = 0.1,\ \ \tau_{23} = 1.0,\ \ \tau_{63} = 0.1,\ \ \tau_{67} = 1.0,\ \ \tau_{75} = 8.0,\\ &\tau_{86} = 1.0,\ \ \tau_{87} = 1.0,\end{aligned} \tag{31}$$

which satisfy Eq. (30). The color of the time series corresponds to that of the oscillators in Fig. 1. The oscillators are uncoupled (i.e., $k = 0$) until $t = 30$ and are then coupled. We can see that the variables converge to the equilibrium point (28) (i.e., $aX_- = 0.0070$).

On the other hand, Fig. 6(b) shows the time series data for the same $k = 1.5$ and connection delays,

$$\begin{aligned}&\tau_{12} = 1.0,\ \ \tau_{21} = 2.0,\ \ \tau_{34} = 4.0,\ \ \tau_{43} = 0.6,\ \ \tau_{54} = 0.2,\\ &\tau_{35} = 0.3,\ \ \tau_{23} = 0.5,\ \ \tau_{63} = 2.0,\ \ \tau_{67} = 0.2,\ \ \tau_{75} = 1.0,\\ &\tau_{86} = 0.7,\ \ \tau_{87} = 0.5,\end{aligned} \tag{32}$$

which also satisfy Eq. (30). Although each delay in Eq. (32) is different from that in Eq. (31), the stability of $g(s)$ for Eq. (32) is equivalent to that for Eq. (31) according to Corollary 1. Figure 6(b) shows the time series data with connection delay

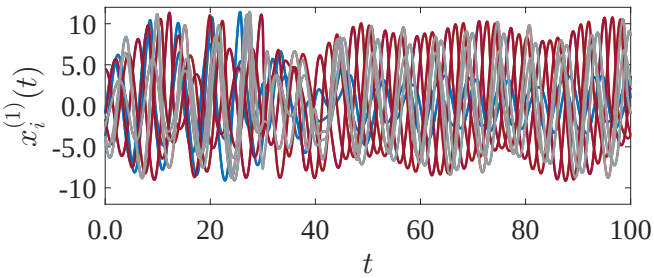

FIG. 7. Time series data for Rössler oscillators with the network topology shown in Fig. 1. The coupling parameters correspond to point A1 in Fig. 4 and point A3 in Fig. 5(a).

(32). The independent oscillators are coupled at $t = 30$. As in Fig. 6(a), all variables converge to aX_- after coupling.

Note that connection delays other than $\tau_{12}, \tau_{21}, \tau_{34}, \tau_{43}, \tau_{54}$, and τ_{35} are set randomly in Eqs. (31) and (32) because they do not affect the stability of steady state (3) (see Corollary 2).

Now we consider the connection parameters corresponding to point A1 in Fig. 4 and point A3: $(\tau_{34} + \tau_{43},\ \tau_{54} + \tau_{43} + \tau_{35}) = (6.0, 6.0)$ in Fig. 5(a). For these parameters, $g_1(s)$ and $H(s) + kL(s)$ in Eq. (29) are stable, but $g_2(s)$ is unstable. Figure 7 shows the time series data for these parameters, in which delays are set as follows: $\tau_{34} = 3.0$, $\tau_{35} = 1.5$, $\tau_{43} = 3.0$, and $\tau_{54} = 1.5$, and the other connection delays are the same as those in Eq. (31). The oscillators are uncoupled for $t \in [0, 30)$, and are coupled at $t = 30$. The variables continue to oscillate after coupling.

Figure 8 shows the time series data with the coupling parameters,

$$(k, \tau_{12} + \tau_{21}, \tau_{34} + \tau_{43}, \tau_{54} + \tau_{43} + \tau_{35}) = (0.5, 1.0, 4.0, 2.0),$$

which corresponds to point B1 in Fig. 4 and point B2 in Fig. 5(b), in which $g_1(s)$ is unstable, whereas $g_2(s)$ and $H(s) + kL(s)$ are stable. As in Figs. 6 and 7, coupling starts at $t = 30$. After coupling, the variables in graph $G^{(\beta)}$ in Fig. 2 (i.e., red and gray) converge to the equilibrium point and those in graph $G^{(\alpha)}$ in Fig. 2 (i.e., blue) oscillate. The above phenomenon can be explained as follows. First, since $g_2(s)$, the characteristic function for graph $G^{(\beta,\beta)}$, is stable, the variables in $G^{(\beta,\beta)}$ converge to the equilibrium point (red in Fig. 8). Second, the stabilized variables of $G^{(\beta,\beta)}$ are input to graphs $G^{(\beta,\alpha)}$ and $G^{(\alpha)}$ through edges containing delays (τ_{63}, τ_{75}) and τ_{23} (see Fig. 1). Then the variables in graph $G^{(\beta,\alpha)}$ (gray in Fig. 8) converge to the equilibrium point. However, the variables in graph $G^{(\alpha)}$ (blue in Fig. 8) still oscillate because $g_1(s)$, the characteristic function for graph $G^{(\alpha)}$ in Fig. 2, is unstable. The main reason for the above phenomenon is that graph $G^{(\beta,\beta)}$ is not affected by other oscillators because of the directional coupling. Thus, this kind of phenomenon may be ubiquitous for directed graphs in which some oscillators are not affected by others.[3]

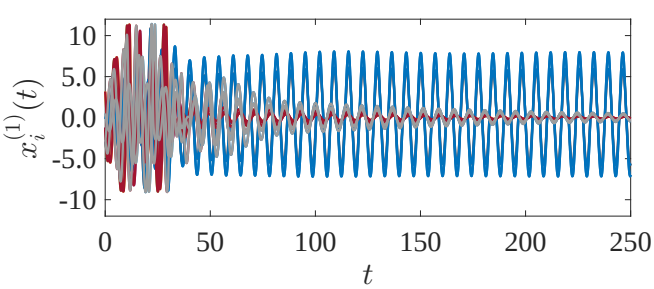

FIG. 8. Time series data for Rössler oscillators with the network topology shown in Fig. 1. The coupling parameters correspond to point B1 in Fig. 4 and point B2 in Fig. 5(b).

One may wonder why all the variables oscillate in Fig. 7 despite $g_1(s)$ being stable. This is because the oscillators in graph $G^{(\alpha)}$ receive the oscillating variable from oscillator 3 in graph $G^{(\beta,\beta)}$, the characteristic function, $g_2(s)$, of which is unstable in Fig. 7.

VI. DISCUSSION

In previous studies [32–36], the componentwise time-shift transformation, which can change connection delays in delay-coupled oscillators without causing qualitative changes in the dynamics, has been proposed to make the analysis easier for the case of heterogeneous connection delays. It has been shown that connection delays in semicycles, which are closed paths in the undirected graph obtained by removing the direction from all the edges in the original graph [33,34], play an important role in the stability analysis. Specifically, as long as the sum of the connection delays in semicycles is preserved, the stability of the steady states does not change regardless of variations in the connection delays. In other words, the stability of the steady states depends on the sum of the connection delays in semicycles. This implies that the number of connection delays to be considered can be reduced while preserving stability by setting the connection delays at certain edges to zero. In particular, for any network topology, the number of connection delays can be reduced by up to $L - N + 1$ without changing the stability, where L is the number of edges [34].

Although the above results based on the componentwise time-shift transformation seem similar to those obtained in the present study in terms of reducing the number of delays for the stability analysis, they differ significantly in the following aspects. In the present study, the stability of the steady states depends on the connection delays in directed cycles in the original graph, which are different from semicycles. For example, in Fig. 1, by focusing on semicycles, we can reduce the number of connection delays to be considered to five on the basis of componentwise time-shift transformation. On the other hand, the present study shows that the number can be reduced to three by focusing on directed cycles as expressed by Eq. (11). Furthermore, the present study shows that decomposition of the characteristic function by removing edges that do not form directed cycles greatly simplifies the analysis. Therefore, our results have the potential to simplify the stability analysis of AD compared to the componentwise time-shift transformation. However, it should be noted that the results reported here apply only to diffusive connections as

[3]This is not partial AD [31], since partial AD is the stabilization of equilibrium points for some oscillators despite the fact that the oscillators are mutually (bidirectionally) coupled to each other.

expressed by Eq. (2), whereas the componentwise time-shift transformation is applicable to a more general class of delayed systems.

VII. CONCLUSION

The present study investigated AD in delay-coupled oscillators on a general directed graph with heterogeneous connection delays. We revealed that the characteristic function for a steady state can be factorized into several functions. These functions correspond to subgraphs in the original graph, which can be obtained by removing all edges that do not form directed cycles in the original graph. Furthermore, we proved that the stability of the characteristic function depends on the sums of the connection delays in the directed cycles in the original graph. It was also shown that the stability is unaffected by connection delays on edges that do not form directed cycles. The above results can significantly simplify the stability analysis of AD, even for a directed graph with heterogeneous connection delays. The theoretical results were validated by numerical simulations using chaotic oscillators.

ACKNOWLEDGMENTS

The present study was supported in part by JSPS KAKENHI (20K19881, 21H03513).

APPENDIX A: PROOF OF LEMMA 1

We consider two cases as follows: (1) a simple situation in which nodes 1 to $N^{(\alpha)}$ belong to subgraph $G^{(\alpha)}$, and nodes $N^{(\alpha)}+1$ to $N^{(\alpha)}+N^{(\beta)}$ belong to subgraph $G^{(\beta)}$ and (2) a more general situation in which node $v_j^{(\alpha)} \in \{1,\dots,N\}$ with $j=1,\dots,N^{(\alpha)}$ is the jth node in $G^{(\alpha)}$ and node $v_i^{(\beta)} \in \{1,\dots,N\}$ with $i=1,\dots,N^{(\beta)}$ is the ith node in $G^{(\beta)}$.

First, we consider case 1. Assume that there exists at least an edge from $G^{(\beta)}$ to $G^{(\alpha)}$, and no edges exist from $G^{(\alpha)}$ to $G^{(\beta)}$. Then matrix $\boldsymbol{E}(s)$ in Eq. (7) is given by

$$\boldsymbol{E}(s) = \begin{pmatrix} \boldsymbol{E}^{(\alpha)}(s) & \boldsymbol{E}_{12}(s) \\ \boldsymbol{0}_{N^{(\beta)}\times N^{(\alpha)}} & \boldsymbol{E}^{(\beta)}(s) \end{pmatrix}, \tag{A1}$$

where $\boldsymbol{E}_{12}(s) \in \mathbb{C}^{N^{(\alpha)}\times N^{(\beta)}}$. Thus, $\hat{g}(s)$ in Eq. (9) is described as

$$\hat{g}(s) = \det\begin{bmatrix} \boldsymbol{I}_{N^{(\alpha)}} - kG(s)\boldsymbol{E}^{(\alpha)}(s) & -kG(s)\boldsymbol{E}_{12}(s) \\ \boldsymbol{0}_{N^{(\beta)}\times N^{(\alpha)}} & \boldsymbol{I}_{N^{(\beta)}} - kG(s)\boldsymbol{E}^{(\beta)}(s) \end{bmatrix}. \tag{A2}$$

Since the lower-left block matrix in Eq. (A2) is a zero matrix, we can factorize Eq. (A2) into two functions as shown in Eq. (12) [see Eq. (2.7.1) in [37]].

Second, we consider case 2. Here $\boldsymbol{E}(s)$ for case 2 is not described by Eq. (A1). However, by interchanging the rows and columns on the right-hand side of Eq. (9), we can rewrite $\hat{g}(s)$ for case 2 as that for case 1 [i.e., Eq. (A2)]. Thus, as in case 1, $\hat{g}(s)$ can be factorized into two functions, as shown in Eq. (12). ■

APPENDIX B: PROOF OF LEMMA 2

Without loss of generality, assume that acyclic graph $G^{(\alpha)}$ consists of nodes $1,\dots,N^{(\alpha)}$ and the indegree of node 1 is 0 [38]. Then the first row of $\boldsymbol{T}^{(\alpha)}(s)$ has all 0 elements, because the first row of the adjacency matrix $\boldsymbol{P}^{(\alpha)}$ for graph $G^{(\alpha)}$ has all 0 elements. Thus, $\boldsymbol{E}^{(\alpha)}(s)$ in Eq. (19) is given by

$$\boldsymbol{E}^{(\alpha)}(s) = \begin{pmatrix} 0 & \boldsymbol{0}_{1,N^{(\alpha)}-1} \\ \boldsymbol{E}_{21}^{(\alpha)}(s) & \boldsymbol{E}^{(\alpha,\beta)}(s) \end{pmatrix}, \tag{B1}$$

where $\boldsymbol{E}_{21}^{(\alpha)}(s) \in \mathbb{C}^{(N^{(\alpha)}-1)\times 1}$. Here $\boldsymbol{E}^{(\alpha,\beta)}(s) \in \mathbb{C}^{(N^{(\alpha)}-1)\times(N^{(\alpha)}-1)}$ contains information about the network topology and the connection delays in graph $G^{(\alpha,\beta)}$, which is obtained by removing node 1 from $G^{(\alpha)}$. Therefore, $g^{(\alpha)}(s)$ in Eq. (13) is described as

$$g^{(\alpha)}(s) = \det\begin{bmatrix} 1 & \boldsymbol{0}_{1,N^{(\alpha)}-1} \\ -kG(s)\boldsymbol{E}_{21}^{(\alpha)}(s) & \boldsymbol{I}_{N^{(\alpha)}-1} - kG(s)\boldsymbol{E}^{(\alpha,\beta)}(s) \end{bmatrix}. \tag{B2}$$

Expanding the first row in Eq. (B2) yields

$$g^{(\alpha)}(s) = g^{(\alpha,\beta)}(s) := \det[\boldsymbol{I}_{N^{(\alpha)}-1} - kG(s)\boldsymbol{E}^{(\alpha,\beta)}(s)].$$

We can see that $g^{(\alpha)}(s)$ corresponding to graph $G^{(\alpha)}$ is equivalent to $g^{(\alpha,\beta)}(s)$ in the remaining graph $G^{(\alpha,\beta)}$. Graph $G^{(\alpha,\beta)}$ is also an acyclic graph [38] and has a node with indegree 0. Thus, by repeatedly expanding the determinant in a similar way to that described above, we obtain $g^{(\alpha)}(s)=1$. ■

APPENDIX C: PROOF OF COROLLARY 1

In this proof, we show that each term obtained by expanding Eq. (9) contains the sum of the connection delays in directed cycles and does not contain each connection delay. In order to calculate Eq. (9), let us define $\hat{\boldsymbol{g}} := \boldsymbol{I}_N - kG(s)\boldsymbol{E}(s)$. According to the definition of the determinant, Eq. (9) can be described as [see, e.g., Eq. (2.7.1) in [37]]

$$\det(\hat{\boldsymbol{g}}) = \sum_{\sigma\in S_\sigma}(-1)^{N_\sigma}\prod_{i=1}^{N}\hat{g}_{\sigma(i),i}, \tag{C1}$$

where $\hat{g}_{\sigma(i),i}$ is the $(\sigma(i),i)$ element of matrix $\hat{\boldsymbol{g}}$. The function σ that reorders the set $\{1,\dots,N\}$ is a permutation of this set (i.e., bijection from $\{1,\dots,N\}$ onto itself). The value in the ith position after reordering by σ is denoted by $\sigma(i)$. Here N_σ is the minimal number of pairwise transpositions needed to transform $\sigma(1),\dots,\sigma(N)$ to $1,\dots,N$, and S_σ denotes the set of all permutations. The following shows that the sums of the connection delays in directed cycles appear in the term $\prod_{i=1}^{N}\hat{g}_{\sigma(i),i}$ in Eq. (C1).

According to the property of permutation σ, in order to calculate the term $\prod_{i=1}^{N}\hat{g}_{\sigma(i),i} = \hat{g}_{\sigma(1),1}\cdots\hat{g}_{\sigma(N),N}$, N elements are selected from $\hat{\boldsymbol{g}}$ so that the column and row numbers do not overlap. Note that the diagonal elements of $\hat{\boldsymbol{g}}$ are $\hat{g}_{\sigma(i),i}=1$ for $i=\sigma(i)\in\{1,\dots,N\}$, whereas the nondiagonal elements are given by $\hat{g}_{\sigma(i),i} = \frac{-kp_{\sigma(i)i}}{d_{\sigma(i)}}G(s)e^{-s\tau_{\sigma(i)i}}$ for $i\neq\sigma(i)$ [see Eq. (9)]. The nondiagonal elements comprise information about the edge from node i to node $\sigma(i)$ (i.e., $p_{\sigma(i)i}$ and $\tau_{\sigma(i)i}$). There are $N!$ permutations of σ in S_σ, i.e., there are $N!$ terms of $\prod_{i=1}^{N}\hat{g}_{\sigma(i),i}$ in Eq. (C1). In the following, we divide $N!$

permutations σ into two cases: (1) $n = 0$ and (2) $n \neq 0$, where n is the number of integers $i \in \{1, \ldots, N\}$ that satisfy $i = \sigma(i)$ in a permutation σ.

1. For σ satisfying $n = 0$ (i.e., $i \neq \sigma(i), \forall i$)

In this case, $\prod_{i=1}^{N} \hat{g}_{\sigma(i),i}$ is calculated by selecting N elements from the nondiagonal elements of $\hat{\boldsymbol{g}}$. Since the nondiagonal elements $\hat{g}_{\sigma(i),i}$ include information about the edge from node i to node $\sigma(i)$, selecting N elements from nondiagonal elements of $\hat{\boldsymbol{g}}$ corresponds to selecting N edges in the graph. Furthermore, these N elements are selected such that the column and row numbers do not overlap. This corresponds to N edges being selected in the graph such that each edge has a different head node and a different tail node. Therefore, N selected edges can only make up directed cycles, in which the indegree and outdegree for all nodes are 1. The term $\prod_{i=1}^{N} \hat{g}_{\sigma(i),i}$ can be calculated as

$$\prod_{i=1}^{N} \hat{g}_{\sigma(i),i} = \frac{\{-kG(s)\}^N}{d_1 \cdots d_N} e^{-s(\tau_{\sigma(1)1} + \cdots + \tau_{\sigma(N)N})}. \tag{C2}$$

Thus, the sums of connection delays in the directed cycles, which are formed by N selected edges, appear in the exponent of Eq. (C2). Note that N selected edges may create multiple independent directed graphs. For this case, the sums of connection delays in the multiple directed cycles appear in the exponent of Eq. (C2).

2. For σ satisfying $n \neq 0$

In this case, there are n integers i that hold $i = \sigma(i)$. Without loss of generality, assume $i = \sigma(i)$ for $i \in \{1, \ldots, n\}$ (i.e., $\sigma(1) = 1, \ldots, \sigma(n) = n$) Since the diagonal elements of $\hat{\boldsymbol{g}}$ are 1, we obtain

$$\prod_{i=1}^{N} \hat{g}_{\sigma(i),i} = \hat{g}_{1,1} \cdots \hat{g}_{n,n} \prod_{i=n+1}^{N} \hat{g}_{\sigma(i),i} = \prod_{i=n+1}^{N} \hat{g}_{\sigma(i),i}. \tag{C3}$$

In order to calculate $\prod_{i=n+1}^{N} \hat{g}_{\sigma(i),i}$, we select $N - n$ elements from nondiagonal elements of the matrix that is obtained by removing the first n rows and columns from $\hat{\boldsymbol{g}}$. This corresponds to selecting $N - n$ edges from a graph that is obtained by removing nodes 1 to n from the original graph. As in case 1, these selected $N - n$ edges form directed cycles in the remaining graph. The right-hand side of Eq. (C3) is calculated as follows:

$$\prod_{i=n+1}^{N} \hat{g}_{\sigma(i),i} = \frac{\{-kG(s)\}^{N-n}}{d_{n+1} \cdots d_N} e^{-s(\tau_{\sigma(n+1)n+1} + \cdots + \tau_{\sigma(N)N})}, \tag{C4}$$

where the exponent includes the sums of the connection delays in the directed cycles in the remaining graph.

From cases 1 and 2, we can confirm that all $N!$ terms of Eq. (C1) include the sums of connection delays in the directed cycles. ■

[1] A. Otto, W. Just, and G. Radons, Philos. Trans. A Math. Phys. Eng. Sci. **377**, 20180389 (2019).
[2] M. K. Stephen Yeung and S. H. Strogatz, Phys. Rev. Lett. **82**, 648 (1999).
[3] M. Kantner, E. Schöll, and S. Yanchuk, Sci. Rep. **5**, 8522 (2015).
[4] T. Banerjee and D. Ghosh, Phys. Rev. E **89**, 052912 (2014).
[5] G. C. Sethia, A. Sen, and F. M. Atay, Phys. Rev. Lett. **100**, 144102 (2008).
[6] G. Saxena, A. Prasad, and R. Ramaswamy, Phys. Rep. **521**, 205 (2012).
[7] W. Zou, D. V. Senthilkumar, M. Zhan, and J. Kurths, Phys. Rep. **931**, 1 (2021).
[8] Y. Sugitani and K. Konishi, NOLTA, IEICE **12**, 612 (2021).
[9] R. Roopnarain and C. S. Roy, Math. Comput. Simul. **187**, 30 (2021).
[10] D. V. Ramana Reddy, A. Sen, and G. L. Johnston, Phys. Rev. Lett. **80**, 5109 (1998).
[11] S. R. Huddy and J. D. Skufca, IEEE Trans. Power Electron. **28**, 247 (2013).
[12] S. K. Subudhi and S. Maity, in *2018 International Conference on Power, Instrumentation, Control and Computing (PICC)* (IEEE, Thrissur, India, 2018), pp. 1–5.
[13] A. Raaj, S. Mondal, and J. Venkatramani, Int. J. Non Linear Mech. **129**, 103659 (2021).
[14] T. Biwa, S. Tozuka, and T. Yazaki, Phys. Rev. Applied **3**, 034006 (2015).
[15] H. Hyodo and T. Biwa, Phys. Rev. E **98**, 052223 (2018).
[16] N. Thomas, S. Mondal, S. A. Pawar, and R. I. Sujith, Chaos **28**, 093116 (2018).
[17] N. Thomas, S. Mondal, S. A. Pawar, and R. I. Sujith, Chaos **28**, 033119 (2018).
[18] A. Sahay, A. Roy, S. A. Pawar, and R. I. Sujith, Phys. Rev. Applied **15**, 044011 (2021).
[19] W. Zou, D. V. Senthilkumar, Y. Tang, and J. Kurths, Phys. Rev. E **86**, 036210 (2012).
[20] R. Xiao, L.-W. Kong, Z.-K. Sun, and Y.-C. Lai, Phys. Rev. E **104**, 014205 (2021).
[21] Y. Sugitani and K. Konishi, Phys. Rev. E **96**, 042216 (2017).
[22] Y. Okigawa, Y. Sugitani, and K. Konishi, Eur. Phys. J. B **93**, 129 (2020).
[23] W. Zou and M. Zhan, Phys. Rev. E **80**, 065204(R) (2009).
[24] K. Konishi, Phys. Rev. E **70**, 066201 (2004).
[25] W. Michiels and H. Nijmeijer, Chaos **19**, 033110 (2009).
[26] F. M. Atay, J. Diff. Equ. **221**, 190 (2006).
[27] W. Zou, D. V. Senthilkumar, M. Zhan, and J. Kurths, Phys. Rev. Lett. **111**, 014101 (2013).
[28] W. Zou, D. V. Senthilkumar, R. Nagao, I. Z. Kiss, Y. Tang, A. Koseska, J. Duan, and J. Kurths, Nat. Commun. **6**, 7709 (2015).
[29] O. E. Rössler, Phys. Lett. A **57**, 397 (1976).
[30] K. Konishi, Phys. Lett. A **341**, 401 (2005).
[31] U. S. Thounaojam and A. Sharma, Chaos Solitons Fractals **124**, 97 (2019).

[32] P. Perlikowski, S. Yanchuk, O. V. Popovych, and P. A. Tass, Phys. Rev. E **82**, 036208 (2010).
[33] L. Lücken, J. P. Pade, K. Knauer, and S. Yanchuk, Europhys. Lett. **103**, 10006 (2013).
[34] L. Lücken, J. P. Pade, and K. Knauer, SIAM J. Appl. Dyn. Syst. **14**, 286 (2015).
[35] A. Wagemakers and M. A. F. Sanjuán, Sci. Rep. **7**, 2744 (2017).
[36] A. Wagemakers, J. Used, and M. A. F. Sanjuán, Eur. Phys. J. Spec. Top. **227**, 1281 (2018).
[37] D. S. Bernstein, *Matrix Mathematics* (Princeton University Press, Princeton, 2009).
[38] J. L. Gross, J. Yellen, and P. Zhang, *Handbook of Graph Theory* (CRC Press, Boca Raton, FL, 2013).